HHS Public Access

Author manuscript

J Magn Reson. Author manuscript; available in PMC 2017 January 01.

Published in final edited form as:

J Magn Reson. 2016 January ; 262: 20–26. doi:10.1016/j.jmr.2015.12.004.

Simultaneous Cross Polarization to ^{13}C and ^{15}N with ^{1}H Detection at 60 kHz MAS Solid-state NMR

Bibhuti B. Das and **Stanley J. Opella***

Department of Chemistry and Biochemistry, University of California, San Diego, La Jolla, California 92093 USA

Abstract

We describe high resolution MAS solid-state NMR experiments that utilize ^{1}H detection with 60 kHz magic angle spinning; simultaneous cross-polarization from ^{1}H to ^{15}N and ^{13}C nuclei; bidirectional cross-polarization between ^{13}C and ^{15}N nuclei; detection of both amide nitrogen and aliphatic carbon ^{1}H; and measurement of both ^{13}C and ^{15}N chemical shifts through multi-dimensional correlation experiments. Three-dimensional experiments correlate amide ^{1}H and alpha ^{1}H selectively with ^{13}C or ^{15}N nuclei in a polypeptide chain. Two separate three-dimensional spectra correlating $^{1}H\alpha/^{13}C\alpha/^{1}H^{N}$ and $^{1}H^{N}/^{15}N/^{1}H\alpha$ are recorded simultaneously in a single experiment, demonstrating that a two-fold savings in experimental time is potentially achievable. Spectral editing using bidirectional coherence transfer pathways enables simultaneous magnetization transfers between ^{15}N, $^{13}C\alpha^{(i)}$ and $^{13}C'^{(i-1)}$, facilitating intra- and inter- residue correlations for sequential resonance assignment. Non-uniform sampling is integrated into the experiments, further reducing the length of experimental time.

Keywords

magic angle spinning; dual observation; peptides; proteins; triple-resonance

Introduction

High-resolution magic angle spinning (MAS) solid-state NMR spectroscopy is in the process of becoming a powerful tool for studying crystalline peptides [1] and proteins [2] as well as proteins immobilized in biological supramolecular assemblies such as membranes [3], fibrils [4], and virus particles [5]. Recent advances include high speed spinning, ^{1}H-detection [6], and non-uniform sampling (NUS) [7–9]. Rapid spinning at the magic angle attenuates the severe line-broadening resulting from the dense $^{1}H/^{1}H$ homonuclear dipole-dipole coupling network present in peptides and proteins. Due to its high gyromagnetic ratio and natural abundance, ^{1}H-detection has been the optimal choice for solution NMR for quite some time, and now with the ability to narrow ^{1}H resonances with fast MAS, it is finding

*Corresponding author: sopella@ucsd.edu.

increasing applications in solid-state NMR. Moreover, NUS can be used to reduce the amount of time required for the experiments.

In addition to detecting and resolving individual resonances, assignment to specific sites is an essential aspect of protein NMR spectroscopy. A number of ^{1}H-detection experiments in solid state have been reported that yield sequence-specific resonance assignments [10, 11] similar to the solution NMR experiment [12]. Current assignment procedures utilize double- and triple- resonance experiments to correlate ^{13}C and ^{15}N chemical shift frequencies with those of amide hydrogens ($^{1}H^{N}$). In contrast to solution NMR experiments, where backbone and side chain ^{1}H, ^{13}C and ^{15}N resonances are assigned using established two- and three-dimensional triple-resonance experiments, in order to measure the chemical shift frequencies of non-amide hydrogens in solid state NMR, four-dimensional experiments or multiple three-dimensional experiments are typically required. For example a four-dimensional experiment correlating ^{1}HXX^{1}H, where X stands for ^{13}C or ^{15}N, has been shown to fully resolve the spectrum of a protein [7]. However, four-dimensional experiments can be extremely time consuming. It is possible for two separate three-dimensional experiments with either ^{13}C or ^{15}N editing to replace four-dimensional experiments, however, this approach can also require long measurement times.

The long times required for the higher dimensional NMR experiments can be addressed by incorporating simultaneous cross-polarization (SIM-CP) from ^{1}H to ^{13}C and ^{15}N sites. Multiple two- and three- dimensional spectra can be obtained from a single experiment in this way [13–16]. These experiments were originally developed for ^{13}C-detection at moderate spinning frequencies. Notably, ^{13}C/^{13}C homonuclear correlation under proton assisted recoupling (PAR) and ^{13}C/^{15}N heteronuclear correlation under proton-assisted insensitive nuclei (PAIN) can be performed using simultaneous spin-lock pulses on three channels under second-order recoupling schemes. In addition, recently, it has been shown that bidirectional cross-polarization between ^{13}C and ^{15}N nuclei can be used to transfer coherence without significant losses in signal intensities [15, 17]. This has enabled triple-resonance experiments to be executed with multiple acquisitions using a single receiver within a single experiment. Further savings of experimental time can be achieved with application of NUS [7, 18–21].

Here we demonstrate ^{1}H-detection experiments that utilize SIM-CP and bidirectional coherence transfer to obtain two separate two- or three- dimensional spectra in a single experiment. These experiments utilize cross-polarization from ^{1}H to both ^{13}C and ^{15}N sites without a substantial loss in sensitivity compared to individual ^{1}H/^{13}C or ^{1}H/^{15}N cross-polarization. Experiments are optimized for bidirectional coherence transfer at 60 kHz MAS in order to transfer magnetization simultaneously and selectively from the amide ^{15}N to the ^{13}Cα of the same residue and the ^{13}C′ of the preceding residue. The experiments also enable sequential homo- and hetero- nuclear correlations between amide ^{1}H and alpha ^{1}H sites to ^{13}C and ^{15}N nuclei in order to improve resolution and to facilitate resonance assignment.

Experimental

Sample preparation

Uniformly ^{13}C and ^{15}N labeled fd bacteriophage with its major coat protein containing the Y21M mutation was obtained using our previously published protocol [5]. Bacteriophage particles from a single batch were concentrated to ~100 mg/ml by ultracentrifugation at 60,000 rpm for 2 hours. The pH of the sample was adjusted to 8.0 using 5 mM sodium borate buffer containing 0.1 mM sodium azide prior to ultracentrifugation. ~30 μL of fully hydrated phage particles at pH 8.0 were transferred to a 1.3 mm zirconium rotor. The sample in the rotor contained ~1 mg of protein.

Uniformly ^{13}C and ^{15}N labeled Met-Leu-Phe tripeptide was purchased from Cortecnet (www.cortecnet.com). ~3.5 mg of microcrystalline peptide was packed in a 1.3 mm MAS rotor.

NMR Spectroscopy

The experiments were performed on a spectrometer with a ^{1}H resonance frequency of 900 MHz. The spectrometer was equipped with a Bruker Avance III HD console and a Bruker 1.3 mm $^{1}H/^{13}C/^{15}N$ triple-resonance MAS probe (www.bruker.com). The spinning rate was controlled at 60.0 kHz. The temperature of the nitrogen gas was maintained at −18° C throughout the experiments. The ^{1}H resonance frequency of water was used to monitor the temperature of the protein-containing sample, and served as an internal chemical shift reference frequency at 4.8 ppm at 20 °C. The chemical shift frequencies of the polycrystalline sample were referenced externally to solid samples with the methylene ^{13}C resonance of adamantane at 38.48 ppm and the ^{15}N resonance of ammonium sulfate at 26.8 ppm [22].

The experimental data were acquired using the pulse sequences diagrammed in Figure 1. Heteronuclear decoupling was accomplished using XiX for ^{1}H [23] and GARP [24] for ^{15}N and ^{13}C nuclei. 30% ramped radio frequency (RF) irradiation on the ^{1}H channel was used for initial cross-polarization (CP) from ^{1}H to ^{13}C, ^{1}H to ^{15}N, and back to ^{1}H during reverse CP. Spin-exchange between ^{15}N and ^{13}C was accomplished using spectrally induced filtering in combination with cross-polarization (SPECIFIC-CP) [25] with 10% ramped amplitude irradiation on the ^{13}C channel. All RF irradiations on the ^{1}H, ^{13}C and ^{15}N channels were matched to the (n-1) Hartmann-Hahn resonance condition for optimal magnetization transfer. The amplitude of the ramped ^{1}H irradiation ranged from 120 kHz to 60 kHz. The ^{13}C and ^{15}N RF amplitudes were adjusted to be near 30 kHz to meet the Hartmann-Hahn condition. Mixing intervals of 1 ms and 0.4 ms were used for initial and final steps in all experiments. A 6 ms mixing time was used to exchange magnetization between ^{15}N and ^{13}C. Phase alternated RF pulses were used to suppress the water signals [26], with 15 kHz RF irradiation for 300 ms. For the fully hydrated biological sample water suppression was improved by increasing the amplitude of the ^{1}H irradiation to ~40 kHz and implementing supercycled phase alternated pulses. All spectra were processed with Bruker TOPSPIN and represented with SPARKY (University of California, San Francisco) programs.

Results

The pulse sequences utilized in this study are diagrammed in Figure 1. All of the experiments were performed with 60 kHz MAS. The sequence for a three-dimensional ^{1}H detection experiment is shown in Figure 1A. One and two-dimensional experiments with ^{1}H detection and simultaneous correlation to ^{13}C and ^{15}N nuclei were adapted from previous publications using simultaneous cross polarization (CP) [14, 15, 17] and concurrent cross polarization pulse schemes [27]. ^{1}H magnetization is transferred to ^{13}C and ^{15}N simultaneously using Hartmann-Hahn CP. Following CP and chemical shift evolution with ^{1}H decoupling, the ^{13}C and ^{15}N magnetizations are stored as Zeeman order using 90° pulses. Water signals and other unwanted ^{1}H signals are suppressed using RF irradiation applied in the XY plane [26]. Then the ^{13}C and ^{15}N magnetizations are flipped back to the transverse direction using 90° pulses. By applying matched RF irradiation on the ^{1}H, ^{13}C, and ^{15}N channels, polarization is transferred back to the ^{1}H nuclei, and subsequently detected under ^{13}C and ^{15}N heteronuclear decoupling.

For heteronuclear correlation, ^{15}N and ^{13}C chemical shift frequencies evolve in the indirect (t_1) dimension under ^{1}H irradiation for decoupling. The chemical shift frequencies are recorded in the phase sensitive mode by incrementing the RF phase by 90° during the initial CP. In one experiment, both ^{13}C and ^{15}N signals are acquired with the same phase. In a second experiment, out of phase signals are acquired by alternating the phase of either the ^{13}C or ^{15}N irradiation by 180°. We have also observed relatively inverted signals (i.e., amide ^{1}H and alpha ^{1}H) by altering the ^{13}C and ^{15}N RF phases during the reverse CP transfer to the ^{1}H nuclei.

Figure 1A illustrates a pulse sequence for a ^{13}C to amide ^{1}H and ^{15}N correlation experiment. The experiment transfers magnetization from ^{1}H to ^{13}C followed by chemical shift evolution in the indirect (t_2) dimension under ^{1}H decoupling. The magnetization from $^{13}C\alpha$ and $^{13}C'$ are transferred selectively to ^{15}N using Hartmann-Hahn CP followed by ^{15}N chemical shift evolution in the indirect (t_1) dimension under ^{1}Hdecoupling. Water resonance suppression pulses are applied before the reverse CP from ^{15}N for ^{1}H-detection.

Three-dimensional correlation experiments with simultaneous ^{13}C and ^{15}N editing were carried out using the pulse scheme shown in Figure 1B. The pulse sequence correlates alpha ^{1}H and amide ^{1}H with either $^{13}C\alpha$ or ^{15}N amide nuclei in a peptide plane. The pulse sequence is similar to that in Figure 1A, except that a spectral editing double cross-polarization between ^{13}C and ^{15}N nuclei is included between the initial and final CP. Both ^{13}C and ^{15}N chemical shift evolutions occur after initial CP. The signals are encoded in the indirect dimensions, and a correlation spectrum of $^{1}H^{N}/^{15}N(^{13}C\alpha)/^{1}H\alpha$ and $^{1}H\alpha/^{13}C\alpha$ $(^{15}N)/^{1}H^{N}$ results.

The spectra shown in Figures 2 and 3 were obtained from a polycrystalline sample of uniformly ^{13}C and ^{15}N labeled Met-Leu-Phe (MLF) peptide utilizing the pulse sequences diagrammed in Figure 1. One-dimensional ^{1}H NMR spectra are shown in Figure 2A–C. Simultaneous observation of amide and aliphatic ^{1}H signals in Figure 2A resulted from using both ^{13}C and ^{15}N editing. The ^{15}N edited amide ^{1}H NMR spectrum is shown in Figure

2B. Similarly the ^{13}C edited aliphatic ^{1}H NMR spectrum in Figure 2C. Notably, all of the magnetization was recovered with simultaneous cross-polarization. Following the one-dimensional experiments, heteronuclear correlation of ^{1}H with ^{13}C and ^{15}N nuclei was obtained by evolving both nuclei simultaneously in the indirect dimension. This is demonstrated with the two-dimensional spectrum shown in Figure 2D, which contains cross-peaks for both ^{13}C and ^{15}N nuclei. The spectrum was obtained with the ^{13}C and ^{15}N magnetization locked with the same phase during Hartmann-Hahn CP. In order to distinguish the chemical shifts by nucleus, two separate data sets were collected. The first experiment was performed using the spin-lock pulses with the same phase. The second data set was acquired with 180° phase shifted ^{15}N spin lock pulses. This resulted in a spectrum where the ^{13}C and ^{15}N cross-peaks are opposite in phase. By adding and subtracting the two data sets, two separate $^{1}H/^{15}N$ and $^{1}H/^{13}C$ heteronuclear correlation spectra are obtained, as shown in Figure 2E and F, respectively. The spectral width/dwell time was kept constant for chemical shift evolution in the indirect dimensions for both ^{13}C and ^{15}N nuclei. However, sensitivity was found to be independent of the dwell times used for each nucleus. A three-dimensional spectrum obtained using different dwell times is shown in Figure 2G. The ^{13}C and ^{15}N spin-lock pulses differed by 180° in phase and the ^{15}N dwell time was set to twice that used for the detection of ^{13}C signals. The cube shows a total of six cross-peaks correlating amide ^{1}H, with alpha ^{1}H, and with ^{15}N amide or $^{13}C\alpha$ chemical shift frequencies. The color codes indicate the signals acquired with opposite phases. The blue and green colors indicate $^{1}H^{N}/^{15}N/^{1}H\alpha$ and $^{1}H\alpha/^{13}C\alpha/^{1}H^{N}$ chemical shift correlation and were generated using $^{1}H^{N}$ (t_2) > ^{15}N (t_1) > $^{13}C\alpha$> $^{1}H\alpha(t_3)$ and $^{1}H\alpha(t_2)$ > $^{13}C\alpha(t_1)$ > N > $^{1}H^{N}$ (t_3) coherence transfer pathways, respectively. Two separate three-dimensional experiments were performed in a similar fashion to that used for the two-dimensional experiments described above. By addition and subtraction of the three-dimensional spectra, separate chemical shift correlation spectra are obtained. The 180° phase shifted spectra are obtained by changing the initial CP irradiation phases followed by chemical shift evolution in the indirect dimension. It is also possible to obtain the phase shifted ^{1}H spectrum with direct detection by changing the phases of the final CP irradiations by 180°.

^{13}C-detected experiments optimized to quantify the magnetization transfer between ^{13}C and ^{15}N at 60 kHz MAS are illustrated in Figure 3. The experiment was carried out using a tailored double CP (DCP) pulse sequence where ^{1}H magnetization is transferred to ^{15}N and subsequently transferred to ^{13}C for detection. During the DCP, no ^{1}H RF irradiation is applied, and the^{13}C spectrum is irradiated at 115 ppm, 55 ppm, or 175 ppm. For specific transfer of ^{15}N magnetization to either $^{13}C\alpha$ or $^{13}C'$, we optimized the experimental conditions in a similar manner as described in an earlier publication [10]. We fixed the ^{15}N and ^{13}C RF amplitudes at 25 kHz and 35 kHz and performed the DCP with the ^{13}C resonance frequency at 55 ppm for $^{13}C\alpha$ and 175 ppm for $^{13}C'$. The RF amplitude applied to ^{13}C was varied to find the maximum sensitivity. Magnetization transfer for $^{13}C\alpha$ only is shown in Figure 3A. For simultaneous magnetization transfer to $^{13}C\alpha$ and $^{13}C'$, we optimized the experiment with fixed RF amplitudes of 15 kHz for ^{15}N and 75 kHz for ^{13}C irradiated at 115 ppm. This is demonstrated in Figure 3B.

One-dimensional results for the MLF tripeptide powder sample, demonstrating the optimal polarization transfer to either carbon or simultaneous selective transfer of magnetization

to $^{13}C\alpha$ and $^{13}C'$, are shown in Figure 3C and D, respectively. For comparison, a spectrum obtained by ^{1}H to ^{13}C direct CP (with a 1 ms mix time) was also obtained (data not shown). All experiments were carried out under similar conditions and the data were processed in the same manner. ^{15}N-edited two-dimensional $^{13}C/^{1}H^{N}$ heteronuclear correlation is shown in Figure 3E. The experiment was carried out using the pulse sequence shown in Figure 1A, except that no ^{15}N chemical shift evolution was incorporated. The peaks are marked for resonances assigned to $^{13}C\alpha$ and $^{13}C'$ chemical shift frequencies of the three amino acid residues.

A three-dimensional experiment correlating the $^{13}C/^{15}N/^{1}H^{N}$ chemical shift frequencies is shown in Figure 3F. The spectrum was obtained using the pulse sequence in Figure 1A and incorporating a 10% non-uniform sampling schedule generated in TOPSPIN and processed using compressed sensing provided in the same software package. The spectrum was reconstructed for a total evolution period of 11 ms ^{1}H (t_3), 6 ms ^{13}C (t_2) and 12 ms ^{15}N (t_1).

The experiments were also applied to a protein sample to demonstrate the breadth of their utility. For this purpose, we used the structural form of the coat protein in fd bacteriophage. NMR signals were obtained from a concentrated solution of uniformly ^{13}C and ^{15}N labeled virus particles. The virus particles are ~90% by weight coat protein subunits, thus the individual signals come from the symmetrically arranged coat proteins. Like wild type fd bacteriophage proteins [28], the mutant Y21M fd coat protein used in these experiments is a 50 amino acid long polypeptide chain with an alpha helical conformation [5]. At 60 kHz MAS, simultaneous CP and ^{1}H detection experiments showed essentially complete polarization transfer similar to that observed for the polycrystalline tripeptide sample. However, due to spectral overlap, only ~30 individual cross-peaks could be identified in the two-dimensional $^{1}H/^{15}N$ heteronuclear single quantum correlation spectrum shown in Figure 4A. Similarly only ~20 cross-peaks could be resolved in the $^{1}H\alpha/^{13}C\alpha$correlation spectrum in Figure 4D. Both spectra were acquired using simultaneous-CP with the pulse sequence shown in Figure 1B. Nearly all protein signals are resolved in the three-dimensional spectra. Two separate three-dimensional correlation spectra such as $^{1}H^{N}/^{15}N/^{1}H\alpha$ and $^{1}H\alpha/^{13}C\alpha/^{1}H^{N}$ were obtained simultaneously using the pulse sequence diagrammed in Figure 1C. Two-dimensional slices correlating $^{1}H/^{13}C$ and $^{1}H/^{15}N$ shifts at various ^{1}H chemical shifts are shown in Figure 4. $^{15}N/^{1}H^{N}$ chemical shift correlation in Figure 4B and C were extracted at 4.2 ppm and 3.8 ppm ^{1}H chemical shift frequencies, respectively. Similarly $^{1}H\alpha/^{13}C\alpha$ two-dimensional planes were obtained at 8.5 ppm and 7.6 ppm $^{1}H^{N}$ chemical shift frequencies. Simultaneous observation of NCO and NCA correlation with $^{1}H^{N}$ detection was carried out using the pulse sequence depicted in Figure 1B. The experiment was carried out in a similar manner to that used for MLF in Figure 3. The two-dimensional plane correlating $^{1}H^{N}$ with ^{13}C shifts in Figure 4G was obtained from the three-dimensional data at 109.7ppm ^{15}N chemical shift.

Discussion

60 kHz MAS enables pulse sequences for simultaneous observation of ^{13}C and ^{15}N signals with ^{1}H detection to be performed. Several pulse sequences were developed with protein

structure determination in mind. In particular, in order to measure ^{1}H chemical shifts in a sequential manner, multiple coherence pathways are used in combination.

Simultaneous cross-polarization transfer enables measurement of the chemical shifts of hydrogens bonded to amide nitrogens and aliphatic carbons. Three resolved amide nitrogen ^{1}H and three alpha carbon ^{1}H resonances are observed in spectra obtained from one-dimensional experiments performed on a polycrystalline sample of the tripeptide MLF, as shown in Figure 2 A–C. Significantly, efficient polarization transfer was achieved using SIM-CP by matching the ^{13}C and ^{15}N RF fields to the (n-1) Hartmann-Hahn resonance condition with ^{1}H.

The two-dimensional correlation spectra in Figure 2D show one-bond correlations of $^{15}N/^{1}H^{N}$ and $^{13}C/^{1}H$ resonances. The residue specific chemical shift assignments were obtained from previously reported ^{13}C-detected experiments [1]. The pulse sequence in Figure 1C enables two separate three-dimensional spectra to be obtained from a single experiment. In particular, these experiments enable the simultaneous observation of ^{13}C and ^{15}N chemical shifts correlated to amide ^{1}H and alpha ^{1}H, in particular $^{1}Hn/N(C\alpha)/^{1}H\alpha$ and $^{1}H\alpha/^{13}C\alpha$ (N)/$^{1}H^{N}$. The advantage of using bidirectional polarization transfer is that amide $^{1}H^{N}$ are correlated selectively with the ^{13}C and/or ^{15}N, and $^{1}H\alpha$ within a residue. This is a prerequisite to assign backbone ^{1}H resonances before they can be correlated to other ^{1}H for assignments and distance measurements.

The experiments simultaneously measure the amide ^{1}H and aliphatic ^{1}H resonance frequencies and have the advantage over conventional methods of using amide ^{1}H-detection only to assign back bone resonances and promote distance measurements through homonuclear spin exchange [14]. This requires multiple step coherence transfers and may cause sensitivity losses for samples that undergo fast relaxation. Secondly, simultaneous ^{13}C and ^{15}N editing experiments may be useful for lifting the ambiguity of resonance assignments for heavily crowded spectra, such as the case shown for fd coat protein.

Additionally, the bidirectional polarization transfer between ^{13}C and ^{15}N has the advantage of correlating amide ^{15}N and $^{13}C\alpha$ chemical shifts within a residue with the $^{13}C'$ chemical shift of the preceding residue. This step of spectral editing/selective magnetization transfer allows the experiment to be used for sequential resonance assignments in proteins. As observed, ^{13}C-detected experiments show nearly 67% and 33% magnetization transfer from ^{15}N to $^{13}C'$ and to $^{13}C\alpha$, respectively. We also observed that the magnetization transfer for the current optimization surprisingly showed 30–50% higher sensitivity compared to the previous optimization method by Barbet-Masin et al. [10] and under similar experimental conditions. Inter- and intra- residue correlation spectra are shown in Figure 3. It is clear from the well-resolved two- and three-dimensional spectra of MLF, which show the amide nitrogen ^{1}H of leucine correlated with the Leu $^{13}C\alpha$ and Met $^{13}C'$ chemical shifts. In the same spectra, the Phe $^{1}H^{N}$ resonance is correlated with its $^{13}C\alpha$ and the Leu $^{13}C'$ chemical shifts. The cross-peaks are marked in Figure 3E by residue type. The three-dimensional data correlating amide ^{15}N and ^{13}C resonances were acquired using a 10% non-uniform sampling schedule in order to reduce the amount of time needed to perform the experiment. The successfully reconstructed spectrum is shown in Figure 3F. The spectrum showed increase

in sensitivity and resolution when compared to the linear method of data acquisition. This was achieved due to the long evolution periods that enabled the line narrowing and improved signal-to-noise ratios. We also performed homonuclear $^{13}C/^{13}C$ mixing prior to heteronuclear $^{13}C/^{15}N$ mixing to simultaneously obtain intra- and inter- residue correlations such as $^{1}H^{N}$/NCACO and $^{1}H^{N}$/NCOCA in a single experiment (data not shown). We note that similar results performed at moderate spinning rate have been recently reported [11].

We also applied the experiments to the 50-residue fd coat protein in intact bacteriophage particles. The heteronuclear correlation spectra in Figure 4A and D contain ~30 distinguishable $^{15}N/^{1}H^{N}$ cross-peaks and ~20 $^{13}C/^{1}H$ cross-peaks, respectively. The relatively narrow spectral dispersion among the alpha hydrogen resonances prevents the two-dimensional from providing unambiguous resolution and assignments. In order to achieve adequate resolution, two separate three-dimensional spectra were acquired in a single experiment using the pulse sequence shown in Figure 1. Two two-dimensional slices correlating amide ^{1}H chemical shifts with ^{15}N chemical shifts obtained at 4.2 ppm and 3.8 ppm ^{1}H chemical shifts are shown in Figure 4B and C, respectively. Similarly, two-dimensional slices correlating alpha carbon ^{1}H resonances with ^{13}C chemical shifts obtained at 8.5 ppm and 7.6 ppm are shown in Figure 4E and F, respectively. We also performed the intra- and inter- residue ^{13}C correlation experiment for fd coat protein similar to the experiment performed on MLF shown in Figure 3D. A representative two-dimensional slice obtained at 109.7 ppm ^{15}N chemical shift is shown in Figure 4G. The spectrum shows Gly23 $^{1}H^{N}$ correlation with Gly23 $^{13}C\alpha$ and Ile22 $^{13}C'$. This experiment is similar to the CANCO type correlation experiment routinely used for resonance assignment in proteins, but with the additional advantage of correlating $^{1}H^{N}$ chemical shifts. As seen from the representative slices, we were able to resolve nearly all resonance peaks and able to assign the proton, carbon and nitrogen chemical shifts for the fd coat protein back bone.

Here we demonstrate that pulse sequences utilizing simultaneous cross-polarization, bidirectional coherence transfer pathways and non-uniform sampling can be used to perform multi-dimensional experiments rapidly and efficiently. We have applied these experiments to fully protonated and uniformly ^{13}C and ^{15}N labeled polycrystalline tripeptide and hydrated bacteriophage samples. Multiple chemical shift correlations are observed using simultaneous CP and bidirectional coherence transfer techniques. Bidirectional CP between inter- and intra- residue ^{13}C and ^{15}N nuclei is efficient under fast MAS and can be exploited further in sequential resonance assignment experiments.

Acknowledgments

The research was supported by grant P41EB002031, R01EB005161, R01GM099986, R01GM066978, and R01AI065361 from the National Institutes of Health. It utilized the Biotechnology Resource Center for NMR Molecular Imaging of Proteins at the University of California, San Diego.

References

1. Rienstra CM, Tucker-Kellogg L, Jaroniec CP, Hohwy M, Reif B, McMahon MT, Tidor B, Lozano-Pérez T, Griffin RG. De novo determination of peptide structure with solid-state magic-angle spinning NMR spectroscopy. Proceedings of the National Academy of Sciences. 2002; 99:10260–10265.

2. Castellani F, van Rossum B, Diehl A, Schubert M, Rehbein H, Oschkinat H. Structure of a protein determined by solid-state magic angle spinning NMR spectroscopy. Nature. 2002; 420:98–102. [PubMed: 12422222]

3. Baker LA, Folkers GE, Sinnige T, Houben K, Kaplan M, van der Cruijsen EA, Baldus M. Magic-angle-spinning solid-state NMR of membrane proteins. Meth Enzymol. 2015; 557:307–328. [PubMed: 25950971]

4. Tycko R, Wickner RB. Molecular structures of amyloid and prion fibrils: consensus versus controversy. Acc Chem Res. 2013; 46:1487–1496. [PubMed: 23294335]

5. Zeri AC, Mesleh MF, Nevzorov AA, Opella SJ. Structure of the coat protein in fd filamentous bacteriophage particles determined by solid-state NMR spectroscopy. Proceedings of the National Academy of Sciences of the United States of America. 2003; 100:6458. [PubMed: 12750469]

6. Zhou DH, Shea JJ, Nieuwkoop AJ, Franks WT, Wylie BJ, Mullen C, Sandoz D, Rienstra CM. Solis-state protein-structure determination with proton-detected triple-resonance 3D magic-angle-spinning NMR spectroscopy. Angew Chemie Intl Ed. 2007; 46:8380–8383.

7. Linser R, Bardiaux B, Andreas LB, Hyberts SG, Morris VK, Pintacuda G, Sunde M, Kwan AH, Wagner G. Solid-State NMR Structure Determination from Diagonal-Compensated, Sparsely Nonuniform-Sampled 4D Proton–Proton Restraints. Journal of the American Chemical Society. 2014; 136:11002–11010. [PubMed: 24988008]

8. Holland DJ, Bostock MJ, Gladden LF, Nietlispach D. Fast Multidimensional NMR Spectroscopy Using Compressed Sensing. Angewandte Chemie International Edition. 2011; 50:6548–6551.

9. Kazimierczuk K, Orekhov VY. Accelerated NMR Spectroscopy by Using Compressed Sensing. Angewandte Chemie International Edition. 2011; 50:5556–5559.

10. Barbet-Massin E, Pell AJ, Retel JS, Andreas LB, Jaudzems K, Franks WT, Nieuwkoop AJ, Hiller M, Higman V, Guerry P, Bertarello A, Knight MJ, Felletti M, Le Marchand T, Kotelovica S, Akopjana I, Tars K, Stoppini M, Bellotti V, Bolognesi M, Ricagno S, Chou JJ, Griffin RG, Oschkinat H, Lesage A, Emsley L, Herrmann T, Pintacuda G. Rapid Proton-Detected NMR Assignment for Proteins with Fast Magic Angle Spinning. Journal of the American Chemical Society. 2014; 136:12489–12497. [PubMed: 25102442]

11. Herbst C, Bellstedt P, Görlach M, Ramachandran R. MAS solid state NMR of proteins: simultaneous 15N–13CA and 15N–13CO dipolar recoupling via low-power symmetry-based RF pulse schemes. Journal of Biomolecular NMR. 2015; 62:7–15. [PubMed: 25712239]

12. Frueh D, Arthanari H, Wagner G. Unambiguous Assignment of NMR Protein Backbone Signals with a Time-shared Triple-resonance Experiment. Journal of Biomolecular NMR. 2005; 33:187–196. [PubMed: 16331423]

13. Nielsen A, Székely K, Gath J, Ernst M, Nielsen N, Meier B. Simultaneous acquisition of PAR and PAIN spectra. Journal of Biomolecular NMR. 2012; 52:283–288. [PubMed: 22371268]

14. Linser R, Bardiaux B, Higman V, Fink U, Reif B. Structure Calculation from Unambiguous Long-Range Amide and Methyl ^{1}H–^{1}H Distance Restraints for a Microcrystalline Protein with MAS Solid-State NMR Spectroscopy. Journal of the American Chemical Society. 2011; 133:5905–5912. [PubMed: 21434634]

15. Das BB, Opella SJ. Multiple acquisition/multiple observation separated local field/chemical shift correlation solid-state magic angle spinning NMR spectroscopy. Journal of Magnetic Resonance. 2014; 245:98–104. [PubMed: 25023566]

16. Herbst C, Herbst J, Leppert J, Ohlenschläger O, Görlach M, Ramachandran R. Chemical shift correlation at high MAS frequencies employing low-power symmetry-based mixing schemes. Journal of Biomolecular NMR. 2011; 50:277–284. [PubMed: 21674236]

17. Gopinath T, Veglia G. Dual Acquisition Magic-Angle Spinning Solid-State NMR-Spectroscopy: Simultaneous Acquisition of Multidimensional Spectra of Biomacromolecules. Angewandte Chemie International Edition. 2012; 51:2731–2735.

18. Hyberts S, Robson S, Wagner G. Exploring signal-to-noise ratio and sensitivity in non-uniformly sampled multi-dimensional NMR spectra. Journal of Biomolecular NMR. 2013; 55:167–178. [PubMed: 23274692]

19. Hyberts SG, Takeuchi K, Wagner G. Poisson-gap sampling and forward maximum entropy reconstruction for enhancing the resolution and sensitivity of protein NMR data. Journal of the American Chemical Society. 2010; 132:2145–2147. [PubMed: 20121194]

20. Palmer MR, Suiter CL, Henry GE, Rovnyak J, Hoch JC, Polenova T, Rovnyak D. Sensitivity of Nonuniform Sampling NMR. The Journal of Physical Chemistry B. 2015; 119:6502–6515. [PubMed: 25901905]

21. Paramasivam S, Suiter CL, Hou G, Sun S, Palmer M, Hoch JC, Rovnyak D, Polenova T. Enhanced Sensitivity by Nonuniform Sampling Enables Multidimensional MAS NMR Spectroscopy of Protein Assemblies. The Journal of Physical Chemistry B. 2012; 116:7416–7427. [PubMed: 22667827]

22. Morcombe CR, Zilm KW. Chemical shift referencing in MAS solid state NMR. Journal of Magnetic Resonance. 2003; 162:479–486. [PubMed: 12810033]

23. Detken A, Hardy EH, Ernst M, Meier BH. Simple and efficient decoupling in magic-angle spinning solid-state NMR: the XiX scheme. Chemical Physics Letters. 2002; 356:298–304.

24. Shaka AJ, Barker PB, Freeman R. Computer-Optimized decoupling scheme for wideband applications and low-level operation. J Magn Reson. 1985; 64:547–552.

25. Baldus M, Petkova AT, Herzfeld J, Griffin RG. Cross polarization in the tilted frame: assignment and spectral simplification in heteronuclear spin systems. Molecular Physics. 1998; 95:1197–1207.

26. Zhou DH, Rienstra CM. High-performance solvent suppression for proton detected solid-state NMR. Journal of Magnetic Resonance. 2008; 192:167–172. [PubMed: 18276175]

27. Leskowitz GM, Ghaderi N, Olsen RA, Mueller LJ. Three-qubit nuclear magnetic resonance quantum information processing with a single-crystal solid. The Journal of Chemical Physics. 2003; 119:1643–1649.

28. Morag O, Sgourakis NG, Baker D, Goldbourt A. The NMR–Rosetta capsid model of M13 bacteriophage reveals a quadrupled hydrophobic packing epitope. Proceedings of the National Academy of Sciences. 2015; 112:971–976.

Highlights

- Bidirectional ^{13}C-^{15}N transfers at 60 kHz
- Simultaneous inter- and intra- residue transfers with ^{1}H irradiation
- Simultaneous acquisition of two three-dimensional spectra with one receiver
- ^{1}H assignments based on bidirectional ^{13}C-^{15}N transfers

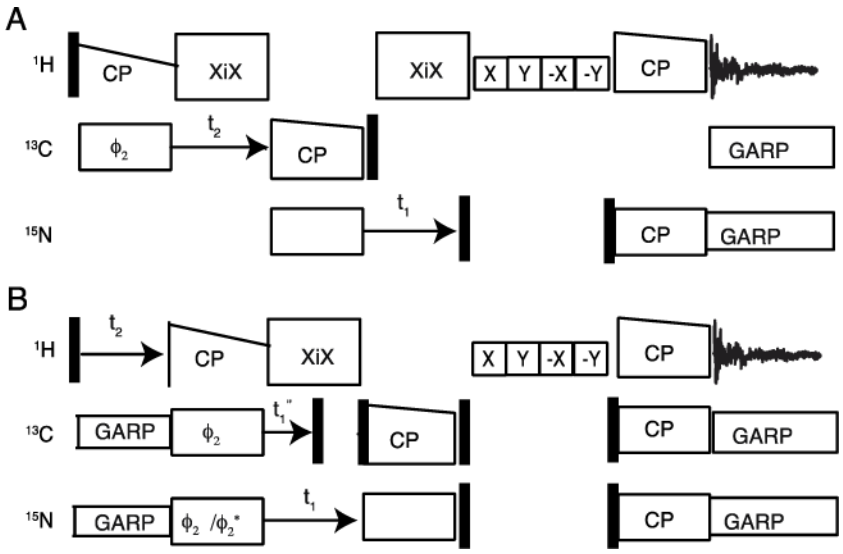

Figure 1.

Three channel pulse sequence diagrams for ^{1}H detection in solid state NMR with 60 kHz magic angle spinning. A. and B. Three-dimensional experiments for simultaneous ^{13}C and ^{15}N edited heteronuclear correlation. A. Experiment for inter and intra residue $^{13}C/^{15}N/^{1}H^{N}$ three-dimensional correlation. B. Experiment for three-dimensional correlation spectroscopy for simultaneous observations of $^{1}Hn/N(C\alpha)/^{1}H\alpha$ and $^{1}H\alpha/^{13}C\alpha(N)/^{1}H^{N}$ resonances. Phase cycling for A ; ^{13}C CP (0 0 0 0 2 2 2 2), ^{13}C and ^{15}N DCP (0), ^{15}N reverse CP (0 0 2 2), ^{1}H reverse CP (0 0 0 0 1 1 1 1 2 2 2 2 3 3 3 3), receiver (1 3 3 1 3 1 1 3 2 0 0 2 0 2 2 0). Phase cycling for B; ^{13}C and ^{15}N CP (0), ^{13}C DCP (0 0 0 0), ^{15}N DCP (0 0 2 2), ^{1}H, ^{13}C and ^{15}N reverse CP (0), receiver (1 3 3 1).

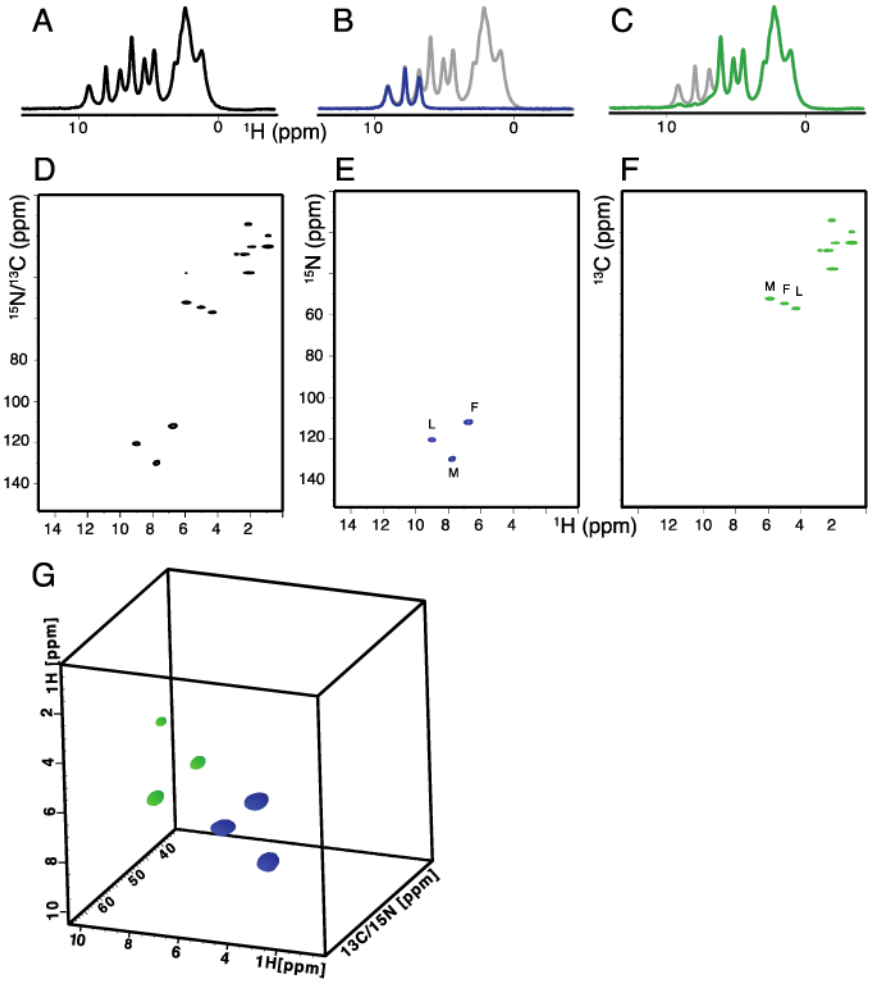

Figure 2.

One-, two-, and three- dimensional spectra of uniformly ^{13}C and ^{15}N labeled polycrystalline Met-Leu-Phe tripeptide obtained with 60 kHz MAS. A.-C. One-dimensional ^{1}H spectra obtained using simultaneous CP. Four scans were co-added for each spectrum. A. ^{13}C and ^{15}N-edited ^{1}H spectrum. B. ^{15}N -edited spectrum. C. ^{13}C edited spectrum. For visual comparison, the one dimensional spectrum from A is plotted in grey in the background. D and E, two-dimensional heteronuclear correlation spectra obtained for a total number of 4 scans. G. Three-dimensional correlation spectrum obtained using the pulse scheme shown in Figure 1C. The color codes are blue for positive and green for negative cross-peaks for ^{1}Hα/^{13}Cα (N)/^{1}H^N and ^{1}Hn/N(Cα)/^{1}Hα correlations, respectively. The three-dimensional data was acquired with a total number of 16 scans; 4 second recycle delay; and evolution periods of 11 ms (t3) ^{1}H, 1.5 ms (t2) ^{13}C, and 2.5 ms (t1) ^{15}N. An equal number of data points were linear predicted during data processing.

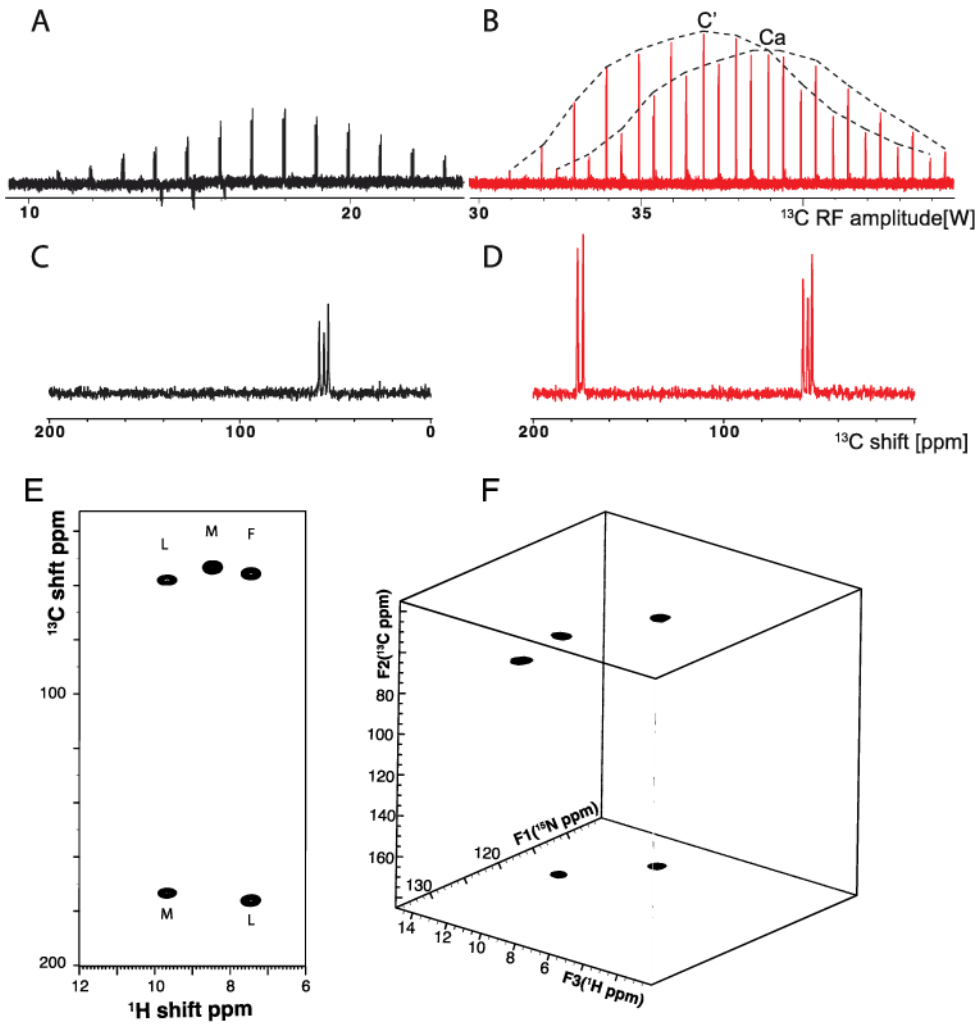

Figure 3.

^{13}C- and ^{1}H- detected spectra of MLF acquired with 60 kHz MAS. A. Variable amplitude ^{13}C spectra of SPECIFIC-CP between ^{15}N and $^{13}C\alpha$ at fixed 25 kHz ^{15}N amplitude. ^{13}C and ^{15}N are irradiated at 55 ppm and 120 ppm respectively. B. Same as A, but ^{13}C irradiated at 115 ppm and ^{15}N amplitude at 15 kHz (2.8 watts). Envelopes on top are drawn to visually guide the magnetization transfer to $^{13}C\alpha$ and $^{13}C'$. C. Optimal 1D spectra obtained from A. D. Same as C, but for ^{13}C amplitude at 38 watts. E. ^{15}N-edited and ^{1}H-detected $^{1}H^{N}/^{13}C$ two-dimensional correlation spectrum. F. ^{1}H-detected $^{13}C/^{15}N/^{1}H^{N}$ three-dimensional correlation spectrum. Both A. and B. were obtained with 16 scans, and 4 second recycle delays. The three-dimensional spectrum was reconstructed from 10% sampling density of a 400 (t2)/64 (t_1) complex data matrix. The sampling schedule was generated in TOPSPIN 3.2 by incorporating T_2 and J coupling values for ^{13}C nuclei. The spectrum was reconstructed using the compressed sensing package in TOPSPIN.

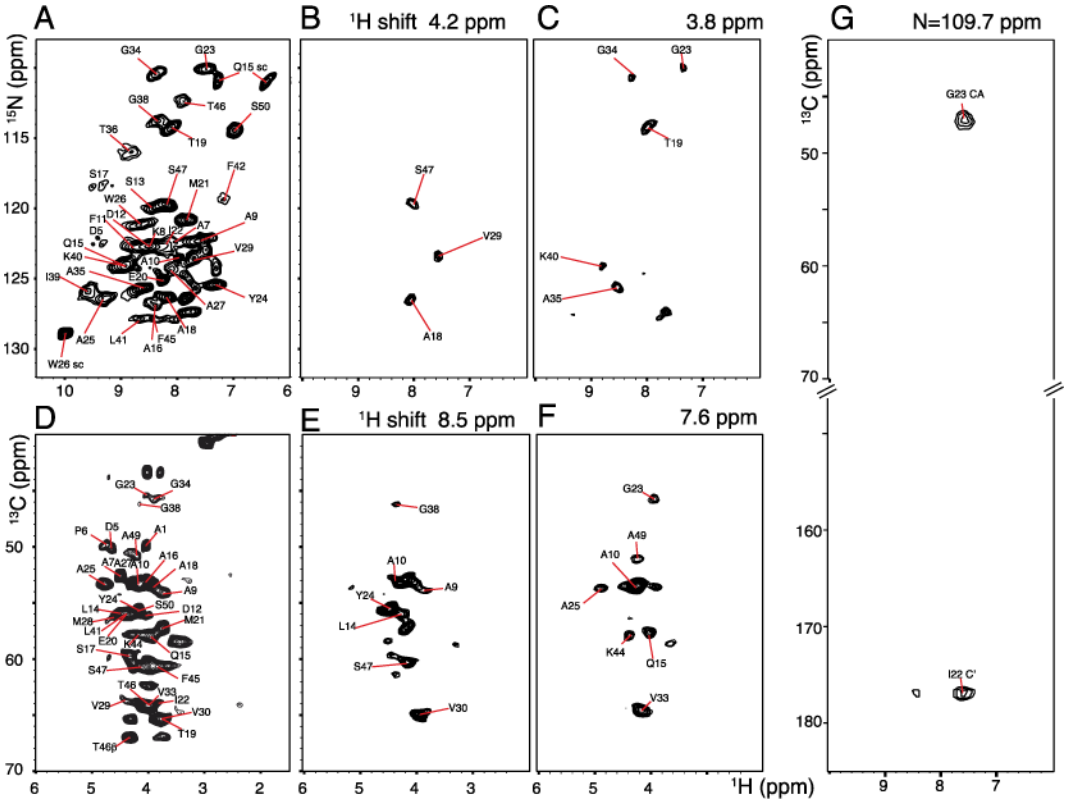

Figure 4.

Two- and three-dimensional spectra of uniformly ^{13}C and ^{15}N labeled fd coat protein in bacteriophage particles obtained with 60 kHz MAS. A. Two-dimensional $^{1}H/^{15}N$ heteronuclear correlation spectrum. B. and C. $^{1}H/^{15}N$ two-dimensional slices obtained at 4.2 and 3.8 ppm ^{1}H chemical shifts, respectively. D. Two-dimensional $^{1}H/^{13}C$ heteronuclear correlation spectrum. E. and F. Two-dimensional slices obtained at 8.5 and 7.6 ppm ^{1}H chemical shifts. A. and D. were obtained using the pulse sequence shown in Figure 1B without incorporating DCP editing pulses. Three-dimensional experiments were carried out using the pulse scheme shown in Figure 1B with a total number of 16 scans, 4 s recycle delay; total evolution periods of 10 ms (t_3) ^{1}H; 3 ms (t_2) ^{1}H; 7.2 ms (t_1) ^{15}N, and 3.6 ms ($t_{1'}$) ^{13}C. Equal numbers of data points were linear predicted during data processing.